

# Stimulus-responsive tumor supramolecular nanotherapeutic system based on indocyanine green

Wenbi Feng<sup>1</sup>, Yuhan Wei<sup>1</sup>, Xianfeng Zhou<sup>2,\*</sup>

<sup>1</sup>School of Polymer Science and Engineering, Qingdao University of Science and Technology, Qingdao, China

<sup>2</sup>School of Materials Science and Engineering, Qingdao University of Science and Technology, Qingdao, China

**Abstract.** Indocyanine green (ICG), a clinical near-infrared fluorescent probe, has the potential to be used as an integrated diagnostic and therapeutic agent for tumors. In this study, ICG-COOH-TK was obtained by connecting ICG molecules through stimulus-responsive thioketone (TK) bond, which can self-assemble into nanoparticles in water. Under 808 nm near-infrared light irradiation, the molecule exhibited excellent photothermal conversion efficiency, as well as better photostability and in vivo circulation stability than free ICG. The nanoparticle can respond to reactive oxygen species (ROS) overexpression in the tumor microenvironment and release ICG upon disassembly, resulting in significantly enhanced fluorescence emission at the tumor. In vitro cell experiments demonstrated excellent biocompatibility and photothermal killing effect on cancer cells, indicating that this molecule can serve as a diagnostic and therapeutic agent for fluorescence-guided tumor photothermal therapy.

## 1. Introduction

Cancer remains one of the deadliest diseases, causing millions of deaths every year [1]. For many cancers, early diagnosis and treatment are crucial for improving survival rates. Fluorescence imaging, with its high sensitivity, low signal-to-background ratio, and real-time detection capabilities, has broad applications in optical therapies for imaging, diagnosis, and treatment [2, 3]. Among many fluorescence imaging techniques, near-infrared (NIR) fluorescence imaging has gained widespread attention due to its rapid, real-time, highly sensitive, and cost-effective advantages [4].

ICG is a commonly used organic dye in NIR fluorescence imaging, with high molar absorption coefficient and excellent biocompatibility. As an US Food and Drug Administration (FDA) approved clinical imaging agent, ICG has strong absorption in the NIR region, high photothermal conversion efficiency, and high biocompatibility, making it a promising agent for cancer diagnosis and therapy [5]. However, maintaining the in vivo stability of ICG is a critical requirement for effective tumor imaging or phototherapy. Free ICG has poor photobleaching resistance after intravenous injection, and it easily binds to plasma proteins and is rapidly cleared from the body, leading to its limited bioavailability at the tumor site, which makes it difficult to achieve specific fluorescence imaging and targeted phototherapy at the tumor site [6]. Furthermore, developing simple fluorescent contrast agents/probes with tumor-specific and high-resolution biological imaging capabilities remains a challenging task, as physically encapsulating and delivering ICG raises complex issues in

pharmaceutical-scale production, drug loading, and potential long-term toxicity [7].

Therefore, based on the heterogeneity of the tumor microenvironment's redox state [8] and the advantages of supramolecular strategies [9], a simple drug delivery system was designed in this study to retain the high biosafety of ICG and expand its potential as a clinical phototherapy agent for near-infrared fluorescence imaging. In this study, an oxidoreductase-responsive connecting linker (TK bond) was used to connect ICG molecules, overcoming the disadvantages of free ICG molecules' poor photobleaching resistance and low tumor targeting ability. At the same time, the introduction of the thioacetal connecting arm improved the hydrophilicity and hydrophobicity of small molecule ICG, allowing it to self-assemble into nano-particles with potential for integrated diagnosis and treatment in water through supramolecular self-assembly. Subsequently, these particles were passively targeted and enriched in tumor tissues through the enhanced permeability and retention (EPR) effect, and under high concentrations of H<sub>2</sub>O<sub>2</sub> in the tumor-specific microenvironment, the TK bond key response was induced to break, releasing small molecule ICG. Under specific excitation wavelengths, it could achieve precise long-term fluorescence imaging of the tumor site with low background and also exhibit precise photothermal therapy effects on the tumor.

\* Corresponding author: [xianfeng@qust.edu.cn](mailto:xianfeng@qust.edu.cn)

## 2. Experimental section

### 2.1 Preparation of ICG-COOH-TK

In this study, a thioketone bonded TK-OH with a double terminated hydroxyl group was first synthesised, then the terminal carboxyl group of ICG was modified to introduce a chemical reaction centre and finally TK-OH was bonded to ICG-COOH by an esterification reaction to give ICG-COOH-TK.

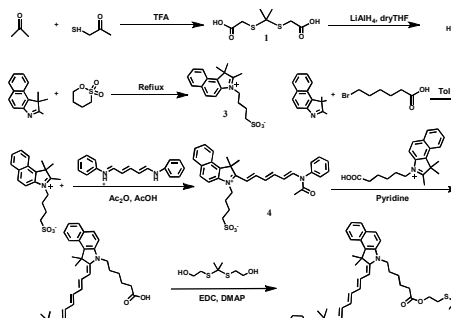


**Figure 1.** Synthetic route of ICG-COOH-TK.

#### 2.1.1 Synthesis of compound TK-OH.

Thioglycolic acid, acetone and trifluoroacetic acid were stirred at room temperature for 4 h. The reaction was quenched by ice water and recrystallized to obtain a white solid compound 1.  $\text{LiAlH}_4$  was dissolved in anhydrous tetrahydrofuran under the protection of nitrogen, and then compound 1 was slowly added to the above solution, and the reaction was quenched by adding deionized water to the system after stirring at room temperature for 10 h. The reaction solution was concentrated by filtration and purified by column chromatography to obtain the oily product TK-OH.

#### 2.1.2 Synthesis of compound ICG-COOH.

The reaction of 1, 1, 2-trimethyl-1H-benzindole with 1, 4-butanedisulfonic acid lactone was carried out at  $120^\circ\text{C}$  for 2 h. The compound 3 was obtained as a light blue solid after extraction and drying. Compound 3 and pentadienyl diphenylamine hydrochloride were added to a mixture of acetic acid and acetic anhydride and refluxed at  $110^\circ\text{C}$  for 2 h. The mixture was concentrated and recrystallized using ether to give purple-red compound 4. 1, 1, 2-trimethyl-1H-benzindole was added to a toluene solution of 6-bromohexanoic acid and refluxed at  $110^\circ\text{C}$  for 24 h. After concentration, compound 5 was obtained as a white solid after washing and drying using deionized water and dichloromethane in turn. Compound 4 and compound 5 were dissolved in the solvent pyridine and refluxed at  $70^\circ\text{C}$  for 2 h. After concentration and recrystallization using ether, the resulting solid was purified by column chromatography to give compound ICG-COOH as a dark green solid.

#### 2.1.3 Synthesis of compound ICG-COOH.

The compound ICG-COOH, EDC, and DMAP were dissolved in dichloromethane. Then add the dichloromethane solution of TK-OH. The reaction was quenched by adding saturated  $\text{NH}_4\text{Cl}$  aqueous solution after stirring for 12 h at room temperature. The extraction was concentrated and purified by column chromatography to obtain the target compound ICG-COOH-TK as a dark green solid.

## 2.2 Characterization of aggregation structure

### 2.2.1 Dynamic light scattering (DLS) characterization.

First, ICG-COOH-TK was dispersed evenly in 2 mL of ultrapure water to prepare a test solution with a final concentration of  $20\ \mu\text{M}$ . Then, the solution was transferred to a quartz cuvette for DLS testing. After being placed in the dark at  $37^\circ\text{C}$  for 24 hours, the sample was measured again under the same testing parameters.

### 2.2.2 Transmission electron microscopy (TEM) characterization.

ICG-COOH-TK was dispersed evenly in ultrapure water to prepare a test solution with a concentration of  $10\ \mu\text{M}$ . After being sonicated to ensure uniform dispersion,  $10\ \mu\text{L}$  of the solution was dropped onto a carbon support film-covered copper grid. After the solvent was allowed to evaporate naturally in the dark, the sample was characterized using TEM.

## 2.3 In vitro photothermal properties

ICG-COOH-TK solutions with concentrations of  $20\ \mu\text{M}$ ,  $40\ \mu\text{M}$ , and  $60\ \mu\text{M}$  were irradiated with a near-infrared laser at a wavelength of 808 nm and a power density of  $2\ \text{W}/\text{cm}^2$ . The temperature of the solution was monitored using a near-infrared thermal imaging system, with readings taken every 10 s and recorded. A photothermal stability experiment was performed on the  $40\ \mu\text{M}$  sample, with the same laser parameters applied for 10 min, and the temperature was recorded every 10 s. The sample was then allowed to cool naturally for 15 min, and the temperature was recorded every 30 s. This cycle was repeated five times.

## 2.4 Stimulus-response characterization study

Using the reported TK oxidation conditions [10], 10 mM  $\text{H}_2\text{O}_2$  was selected as the target ROS concentration.  $10\ \mu\text{M}$  ICG-COOH-TK was co-incubated with 10 mM  $\text{H}_2\text{O}_2$  in ultra-pure water at  $37^\circ\text{C}$  in the dark for 24 hours. The UV-Vis absorption spectra and fluorescence emission spectra of  $10\ \mu\text{M}$  ICG-COOH-TK nanoparticles in aqueous solution before and after  $\text{H}_2\text{O}_2$  response were studied.

## 2.5 Evaluation of cytotoxicity and in vitro photothermal properties on tumor cells

The Live/Dead dual staining method was used to evaluate cell viability through imaging. First, Hela cells in logarithmic growth phase were digested and counted, and 104 cells were seeded in two 96-well plates (light toxicity group and dark toxicity group) and incubated at 37°C in a cell culture incubator for 24 hours until the cell fusion rate reached 70%-80%. ICG-COOH-TK concentration gradients ranging from 0.2  $\mu\text{M}$  to 100  $\mu\text{M}$  were prepared by serial dilution, and four replicate wells were prepared for each concentration gradient. After co-incubation for 24 hours, the light toxicity group was exposed to an 808 nm laser (2 W/cm<sup>2</sup>) for 6 minutes per well, while the dark toxicity group was not treated. After irradiation, the original medium was replaced with fluorescent staining solutions with Calcein-AM and EthD-1 concentrations of 2  $\mu\text{M}$  and 4  $\mu\text{M}$ , respectively, and incubated for 30 min. Finally, the stained cells were observed under a fluorescence microscope.

## 3. Results and Discussion

### 3.1 Characterization of supramolecular aggregation structure of ICG-COOH-TK nanoparticles

DLS can calculate the information of nanoparticle particle size and its distribution by measuring the change of light intensity fluctuation of the laser beam through the nanoparticles. As shown in Figure 2 (a), ICG-COOH-TK formed nanoclusters with hydrodynamic size of about 120 nm by supramolecular self-assembly in water, which were located in the suitable particle size range for passive targeting drug delivery. No significant changes in nanoparticle size were observed after 24 h of placement, and only a slight broadening of the particle size distribution was observed, demonstrating that the ICG-COOH-TK nanoparticles have good size stability in water. According to the TEM results in Figure 2 (b), it can be seen that ICG-COOH-TK formed spherical nanoaggregates in water and the particle size matched with the hydrodynamic size results obtained from DLS characterization, further demonstrating that ICG-COOH-TK can self-assemble in aqueous solution to form nanoparticles with size supporting the EPR effect.

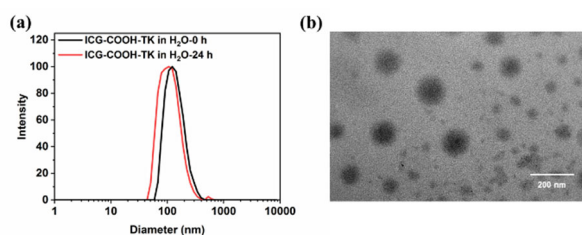


**Figure 2.** (a) DLS results of ICG-COOH-TK nanoparticles placed in water for 0 h and 24 h (b) TEM image of ICG-COOH-TK nanoparticles.

### 3.2 Photothermal effect of ICG-COOH-TK nanoparticles

The heating results at different concentrations are shown in Figure 3 (a). The test solution at 60  $\mu\text{M}$  reached a high temperature of 37.3°C after 10 min of irradiation, while the test solutions at 40  $\mu\text{M}$  and 20  $\mu\text{M}$  heated up to 31.6°C and 21.4°C, respectively. In contrast, ultrapure water showed only a slight temperature change, heating up by less than 2°C under the same conditions. This demonstrates that ICG-COOH-TK nanoparticles have a good photothermal effect in water and confirms their potential as photothermal agents for PTT therapy. The results of the photothermal stability experiment are shown in Figure 3 (b). Five cycles of heating and cooling showed that although the photothermal stability of the sample slightly decreased after cycling, each laser irradiation still caused the sample to heat up by at least 19°C from room temperature. This demonstrates that the sample can still release stable photothermal effects during repeated heating and cooling cycles, indicating excellent photothermal stability.

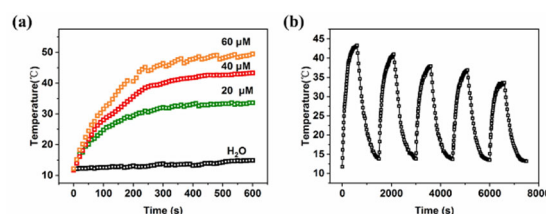


**Figure 3.** (a) Temperature elevation profiles of ICG-COOH-TK nanodisc in aqueous solution at different concentrations (2 W/cm<sup>2</sup>, 808 nm) (b) The heating/cooling curves of ICG-COOH-TK nanodiscs (20  $\mu\text{M}$ ) in water for continuous five cycles.

### 3.3 Characterization of ICG-COOH-TK after ROS stimulation response

As shown in Figure 4 (a), the UV-Vis absorption spectrum of ICG-COOH-TK nanoparticles displayed enhanced absorption and a narrower peak at around 780 nm after the cleavage of TK bond by H<sub>2</sub>O<sub>2</sub>, compared to the spectrum before the response. This is due to the disappearance of the aggregation structure of the nanoparticles after the response, leading to more excellent optical properties. Moreover, as seen in Figure 4 (b), the fluorescence emission spectrum after H<sub>2</sub>O<sub>2</sub> response was greatly enhanced, with the maximum emission wavelength located at around 816 nm. The fluorescence intensity increased sharply from almost baseline to  $5.95 \times 10^4$ , indicating the recovery of fluorescence quenching caused by aggregation due to the disintegration of the nanoparticles after the cleavage of the TK bond.

The change in optical properties after ROS response enables ICG-COOH-TK nanoparticles to respond to stimuli in high ROS concentration environments after targeted delivery to tumors, exhibiting enhanced fluorescence imaging at the tumor site. This improves the limited imaging resolution caused by aggregation-induced quenching and facilitates high contrast imaging-guided photothermal therapy, making it favorable for application in imaging-guided cancer treatment.

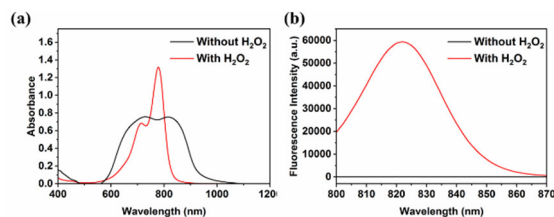


**Figure 4.** UV absorption spectra (a) and fluorescence emission spectra (b) of ICG-COOH-TK before and after the ROS response.

### 3.4 In vitro biocompatibility and photothermal cytotoxicity of ICG-COOH-TK

As shown in Figure 5, ICG-COOH-TK exhibited nearly 100% cancer cell photothermal ablation efficiency at a concentration of 12.5  $\mu\text{M}$  after light irradiation, as evidenced by the significant red fluorescence of dead cells, demonstrating the excellent photothermal therapeutic potential of ICG-COOH-TK in cells. The corresponding sample showed low dark toxicity at this concentration, and no significant cytotoxicity was observed in the absence of external near-infrared light irradiation, with cells showing extensive green fluorescence, indicating that ICG-COOH-TK maintains the high biocompatibility advantages of free ICG. The simple molecular design makes it biocompatible and safe.

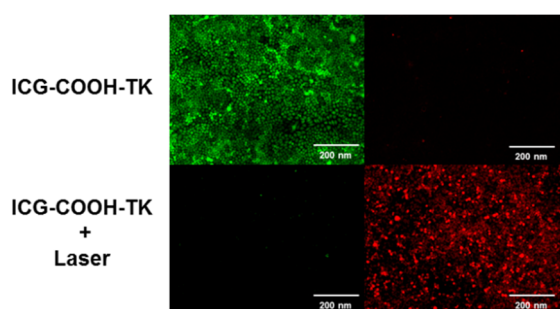


**Figure 5.** In vitro dark toxicity and photothermal effects of ICG-COOH-TK on HeLa cells.

## 4. Conclusion

In this study, we combined the redox heterogeneity of the tumor microenvironment with the advantages of supramolecular strategy to synthesize ICG-COOH-TK, a nano-therapeutic integrated molecule composed of ICG molecules linked by thioketone bonds. The introduction of stimulus-responsive linkages allows target molecules to form nanoclusters through supramolecular self-assembly, improving photostability and photothermal conversion efficiency, extending in vivo circulation time and improving tumor targeting. We have also demonstrated through in vitro cellular experiments that the nanoparticles can respond to excess ROS in the tumour microenvironment and release ICG, enabling enhanced fluorescence imaging and precise photothermal treatment of tumour sites while providing excellent biosafety.

## References

1. Khalil, D. N.; Smith, E. L.; Brentjens, R. J.; Wolchok, J. D., The future of cancer treatment: immunomodulation, CARs and combination immunotherapy. *Nature Reviews Clinical Oncology* 2016, 13 (5), 273-290.
2. Cheng, L.; Yuan, C.; Shen, S.; Yi, X.; Gong, H.; Yang, K.; Liu, Z., Bottom-up synthesis of Metal-Ion-Doped WS<sub>2</sub> nanoflakes for cancer theranostics. *ACS Nano* 2015, 9 (11), 11090-11101.
3. Son, J.; Yi, G.; Yoo, J.; Park, C.; Koo, H.; Choi, H. S., Light-responsive nanomedicine for biophotonic imaging and targeted therapy. *Advanced Drug Delivery Reviews* 2019, 138, 133-147.
4. Kim, H.; Beack, S.; Han, S.; Shin, M.; Lee, T.; Park, Y.; Kim, K. S.; Yetisen, A. K.; Yun, S. H.; Kwon, W.; Hahn, S. K., Multifunctional photonic nanomaterials for diagnostic, therapeutic, and theranostic applications. *Advanced Materials* 2018, 30 (10), 1701460.
5. Lau, C. T.; Au, D. M.; Wong, K. K. Y., Application of indocyanine green in pediatric surgery. *Pediatric Surgery International* 2019, 35 (10), 1035-1041.
6. Liu, R.; Tang, J.; Xu, Y.; Zhou, Y.; Dai, Z., Nano-sized indocyanine green J-aggregate as a one-component theranostic agent. *Nanotheranostics* 2017, 1 (4), 430-439.
7. Reis, C. P.; Neufeld, R. J.; Ribeiro, A. J.; Veiga, F., Nanoencapsulation I. Methods for preparation of drug-loaded polymeric nanoparticles. *Nanomedicine: Nanotechnology, Biology and Medicine* 2006, 2 (1), 8-21.
8. Peng, S.; Xiao, F.; Chen, M.; Gao, H., Tumor - microenvironment - responsive nanomedicine for enhanced cancer immunotherapy. *Advanced Science* 2022, 9 (1), 2103836.
9. Ma, X.; Zhao, Y., Biomedical applications of supramolecular systems based on host-guest interactions. *Chemical reviews* 2015, 115 (15), 7794-7839.
10. Pei, Q.; Hu, X.; Zheng, X.; Liu, S.; Li, Y.; Jing, X.; Xie, Z., Light-activatable red blood cell membrane-camouflaged dimeric prodrug nanoparticles for synergistic photodynamic/chemotherapy. *ACS Nano* 2018, 12 (2), 1630-1641.